Micro- and nanoscale domain engineering in lithium niobate and lithium tantalate

Vladimir Ya. Shur*[a], Evgenii Rumyantsev[a], Ekaterina Nikolaeva[a], Eugene Shishkin[a]

Robert G. Batchko[b], Gregory D. Miller[b], Martin M. Fejer[b], Robert L. Byer[b]

[a]Inst. of Phys. & Appl. Math., Ural State Univ., Ekaterinburg 620083, Russia

[b]E.L. Ginzton Laboratory, Stanford University, Stanford, CA 94305-4085

ABSTRACT

We present detail investigation of the domain evolution in lithium niobate and lithium tantalate during backswitched electric field poling which allowed to produce micro- and nanoscale domain patterns by application of voltage to lithographically defined strip electrodes. *In situ* optical observation of the domain kinetics during poling and high-resolution visualization by SEM and SFM of the static domain patterns on polar surfaces and cross-sections have been used. We separated and studied the main stages of domain evolution. The important role of backswitching as a powerful tool for high-fidelity domain patterning in thick wafers and for production of quasi-periodic nanoscale domain patterns has been demonstrated. We have proposed several variants of domain manipulation during backswitched poling: the frequency multiplication of the domain patterns, domain "erasing" and "splitting", formation of oriented arrays of nanoscale domains. We have demonstrated the production of lamellar domain patterns with period down to 2.6 microns in 0.5-mm-thick wafers and strictly oriented quasi-periodic domain arrays consisting of the individual nanodomains with diameter down to 30 nm and density up to 100 per square micron.

Keywords: domain patterning, backswitching, nanotechnology, electric field poling, domain manipulation.

1. INTRODUCTION

In recent years rapid development of a new branch of technology named the microdomain engineering raised the questions of fabrication of ferroelectric domain patterns with periods about several microns. The solving of this problem is a critical step in the improvement of characteristics of electro-optical and nonlinear optical devices. The new class of engineerable nonlinear optical materials is widely used for the development of wide range of tunable coherent light sources based on quasi-phase matching.[1] Lithium niobate $LiNbO_3$ (LN) and lithium tantalate $LiTaO_3$ (LT) are the most important representatives of this class due to large electro-optical and nonlinear optical coefficients. The new method based on the application of electric field through lithographically defined electrodes for domain patterning allows the production of available devices for wide usage.[2] However the extremely high coercive voltage and the impeding effect of domain spreading out of the electroded area impose problems in obtaining the short-pitch domain patterns. We report the results of the experimental study, which allow this obstacle to be overcome and present the first results on nanoscale domain engineering. The knowledge of the physical principles of the formation of "super-short" domain patterns in thick wafers of such "inconvenient" materials as "the frozen ferroelectrics" LN and LT opens wide perspectives in other ferroelectrics.

2. PERIODICAL DOMAIN PATTERNING IN LITHIUM NIOBATE AND LITHIUM TANTALATE

2.1. Fabrication of periodically poled congruent lithium niobate and lithium tantalate

Periodic domain structures were prepared in optical-grade single-domain 0.5-mm-thick LN and 0.3-mm-thick LT wafers of congruent compositions cut perpendicular to polar axis. The wafers were lithographically patterned with periodic strip metal (NiCr) electrodes deposited on $\mathbf{Z}^+$ surface only. Electrodes in LN were oriented strictly along one of **Y** axis. Patterned surface was covered by a thin (about 0.5-μm thick) insulating layer (photoresist or spin-on-glass) (Fig. 1a). For *in situ* investigation of domain kinetics in uniform electric field we used 1-mm-diameter circular transparent electrodes of two types: 1) liquid electrolyte (LiCl water solution) in special fixture, and 2) In_2O_3:Sn films deposited by magnetron sputtering.

* Correspondence: Email: vladimir.shur@usu.ru; WWW: http://www2.usu.ru/ipham/LabFer; Telephone: 7(3432)617 455; Fax: 7(3432)615 978

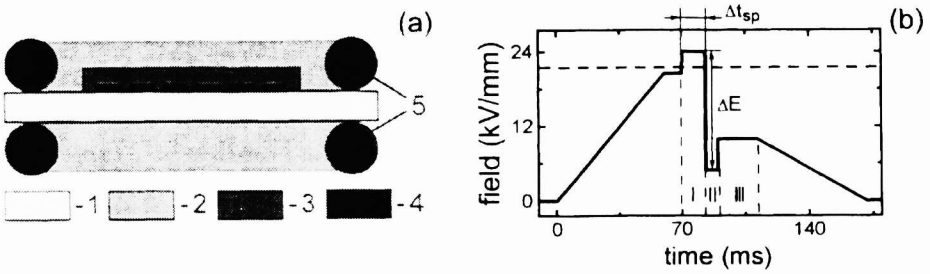

Fig. 1 (a) Scheme of experimental setup: 1 - $LiNbO_3$ wafer, 2 - liquid electrolyte, 3 - insulating layer, 4 - periodic electrodes, 5 - O-rings. (b) backswitched poling voltage waveform: I - high-field stage, II - low-field stage, III - stabilization stage.

A high voltage pulse producing an electric field greater than the coercive field (E_c = 21.5 kV/mm) was applied to the structure through the fixture containing a liquid electrolyte (LiCl).[3,4] The waveform for backswitched poling consisted of three levels of external field: "high field", "low field" and "stabilization field" (Fig. 1b). The switching from single domain state took place at "high field" and the backswitching (flip-back)[5-8] occurred at "low field". The crucial parameters for backswitching kinetics were the duration of the "high field" stage Δt_{sp} and the field diminishing amplitude ΔE. The domain patterns obtained for the different duration of the "low field" stage yielded information about the domain structure development during backswitching. For observation of the domain patterns after partial poling **Z** surfaces and polished **Y** cross-sections were etched for 5-10 min by hydrofluoric acid without heating.[4] The obtained surface relief was visualized by optical microscope, and by scanning electron microscopy (SEM) and force microscopy (SFM). Moreover we carried out direct observations of the domain evolution using a polarizing microscope with simultaneous TV recording and image processing. We investigated 0.2 mm-thick wafers of LN with liquid electrolyte electrodes on both sides. This technique allows direct information to be obtained about the reconstruction of the domain shape and to obtain the field dependence of the sideways wall motion velocity, which is of principal importance for optimization of the poling voltage waveform.

2.2. Domain shape during patterning in lithium niobate and lithium tantalate

The patterning under the periodic strip electrodes provides the anisotropic conditions for domain growth. Therefore the typical domain patterns contain the domains with all walls oriented strictly along the **Y** directions, but not the regular hexagons (Fig. 1a). The domains which appears as a result of switching in stronger fields sometimes demonstrate the triangular shape with domain walls oriented along **X** directions only (Fig. 1b). This situation is similar to the effect of the influence of the field on the domain shape, which have been discovered by us in $Pb_5Ge_3O_{11}$.[9]

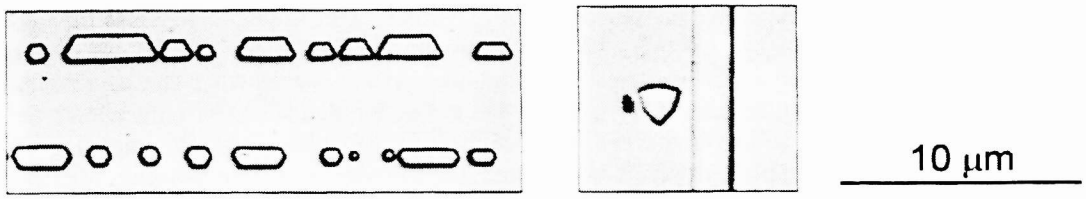

Fig. 2 (a) Typical and (b) triangular domains at Z^- surface in LN. Patterns revealed by etching and visualized by optical microscopy.

The problem of formation of plane domain walls in LT is more complicated than in LN due to triangular shape of individual domains. We carried out the observation of a great number of periodical short-pitch domain patterns in LT. The typical results of domain wall formation on Z^- surface for 2.6-μm period is presented in Figure 2. Usually the individual domains do not merge (Fig. 2a). In the case of merging formed strip domains have only one plane wall (Fig. 2b). The rare strip domains with both plane walls were never obtained for short-pitch patterning without local loosing of periodicity (Fig. 2b).

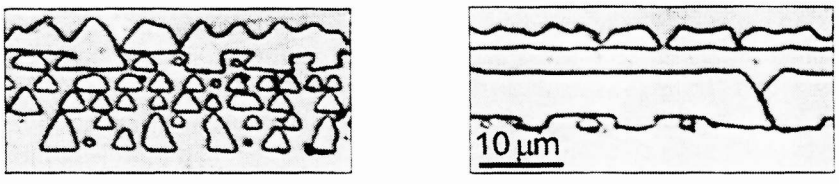

Fig. 3 Domain patterns in LT. Z^- view. Domain patterns revealed by etching and visualized by optical microscope.

3. SPREADING OF THE DOMAIN WALLS OUT OF THE ELECTRODES IN LITHIUM NIOBATE

One of the most important problems of periodic domain patterning is the essential domain spreading out of electroded area. The process leads to uncontrolled variation of the duty cycle and even to merging of the domains especially for short-pitch domain patterns. We have determined that rarely observed finger-assisted self-maintained mechanism of domain wall motion is the most unpleasant.

3.1. Finger-assisted domain wall motion

The scenario of the abnormal domain wall evolution during spreading in LN was investigated using the tilted cross-sections (Fig. 4), which provides the time dependence of the wall structure. One can observe: 1) arising of periodic irregularities (Fig. 4a), 2) growth of oriented "fingers" (Fig. 4b,c), 3) merging of neighboring fingers (Fig. 4d,e,f). It must be pointed out that this process results in the anomaly large shift of the domain walls out of the electroded area.

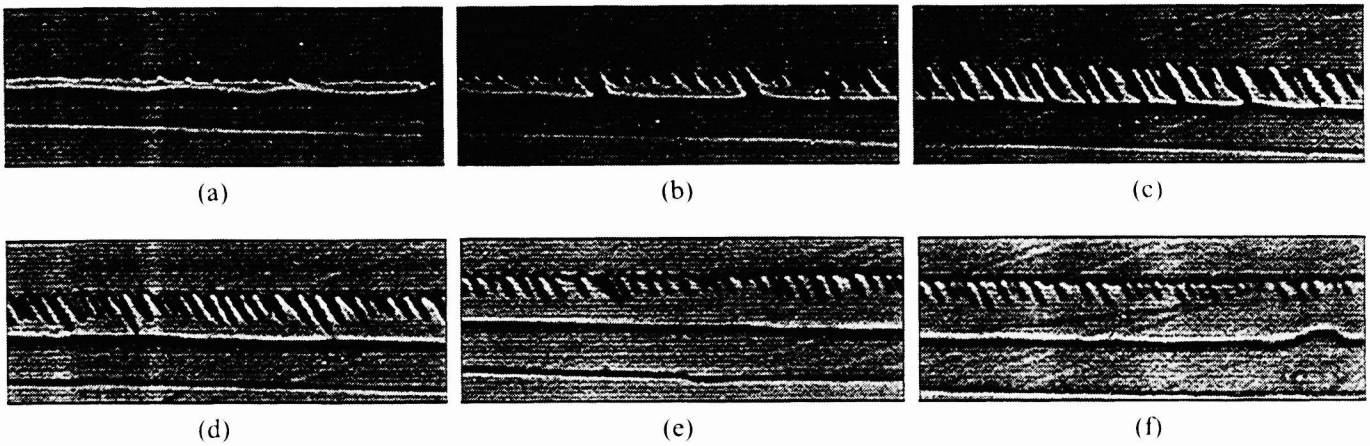

Fig. 4 Stages of the domain wall evolution during finger-assisted spreading out of electrodes in LN. Domain patterns on tilted cross-section were revealed by etching and visualized by optical microscopy.

3.2. Calculation of the domain wall spreading out of the electroded area

Spreading of the formed domain walls out of electrodes for thick sample (the electrode period $\Lambda << \mathbf{d}$) can be considered as a domain wall motion in uniform electric field. It is clear that the spatial inhomogeneity of external field $\mathbf{E_{ex}}$, which is so important for nucleation, exists only in the surface layer with the thickness of about several Λ.

The wall velocity is determined by the polar component of the local electric field $\mathbf{E_z}$.[10] The ratio of compensation of depolarization field by external screening in the area between metal electrodes by charge redistribution at the liquid electrodes is smaller as compare with the compensation under the metal electrodes (Fig. 5). This effect and comparatively slow bulk screening in LN at room temperature lead to decrease of $\mathbf{E_z}$ during shifting due to increasing of uncompensated part of depolarization field. The domain wall stops when

$$E_z(\Delta x) - E_{st} \sim 0 \qquad (1)$$

where $\Delta \mathbf{x}$ – shift of the domain wall out of electrode.

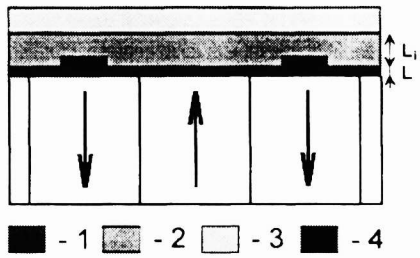

Fig. 5 Scheme of the substrate surface region (1 – dielectric gap, 2 – insulating layer, 3 – liquid electrolyte, 4 – metal electrodes).

Assuming that conductivity of insulating layer and bulk screening can be ignored and that the thickness of insulating layer $\mathbf{L_i} >> \mathbf{L}$, the dependence of average bulk value of $\mathbf{E_z}$ on $\Delta \mathbf{x}$ for used experimental setup (Fig. 5) can be estimated. As the electrode period Λ is very small in comparison with the sample thickness $\mathbf{d}$ the depolarization field is assumed to be spatially uniform and approximated by field in capacitor with effective charge equal to the sum of non-compensated charges at the nonelectroded area and the dielectric permittivity of the insulating layer ε_i.

$$E_{dr}(\Delta x) = (2P_s/\varepsilon_o\varepsilon_i)\,(L_i/d)\,(2\Delta x/\Lambda) \qquad (2)$$

The decrease of $\mathbf{E_z}$ during wall motion occurs due to the increasing of depolarization field $\mathbf{E_{dr}(\Delta x)}$ and the field produced by the "frozen" bulk screening charges (memory effect).

Taking into account the experimentally obtained field dependence of the domain wall velocity for periodical switching the simulation of the switching process was carried out. Time dependence of the sideways domain wall velocity was obtained (Fig. 6a).

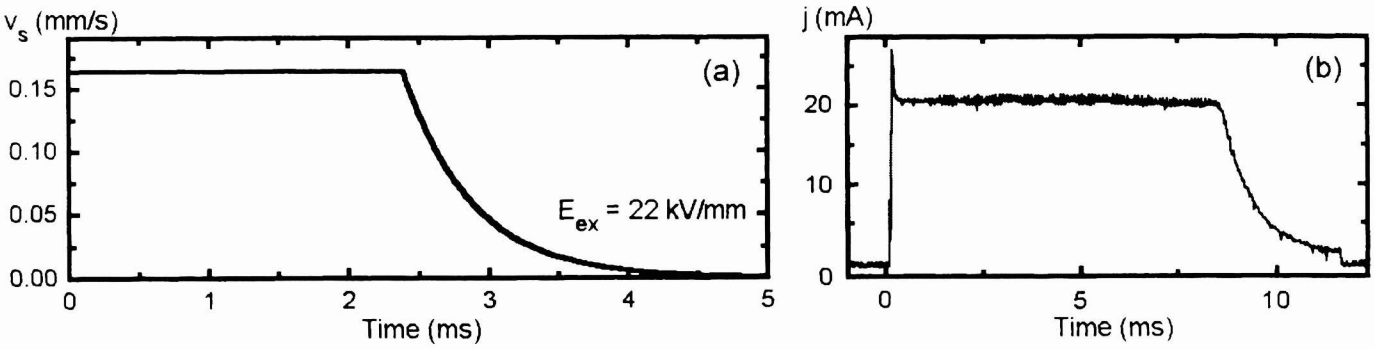

Fig. 6 (a) Simulated time dependence of the sideways domain wall motion velocity, (b) experimental switching current.

The similarity of the simulated wall velocity time dependence (Fig. 6a) and the experimental switching current data (Fig. 6b) shows that the proposed model can be successfully used to describe the domain wall motion out of electrodes during periodical patterning.

3.3. Domain walls interaction during coalescence

The complete merging of the neighboring domain walls as a result of domain spreading out of electrodes is essentially unpleasant for short pitch patterning. It is clear that depolarization field produced by the neighboring domain influences the domain walls motion. When the walls come together the depolarization field doubles and the velocity of the domain wall decreases. Examples of the domain-domain interaction can be seen in Figure 7.

The conditions for coalescence of the domain walls at $\mathbf{Z^+}$ and $\mathbf{Z^-}$ surfaces differ essentially due to different electrode configurations. Domain walls at $\mathbf{Z^-}$ surface move in uniform field with fast enough screening. Therefore even just before coalescence distance between them is uniform and residual narrow domain vanishes uniformly (Fig. 7a).

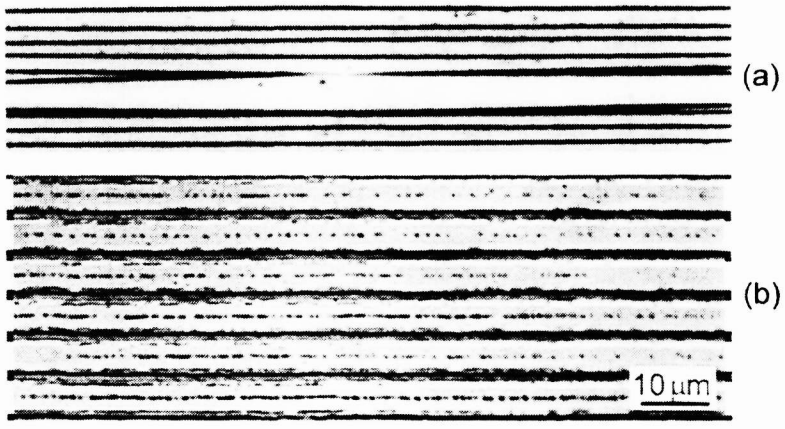

Fig. 7 Domain walls coalescence out of electrodes in LN (a) at $\mathbf{Z^-}$ surface; (b) at $\mathbf{Z^+}$ surface. Black rectangles show the positions of electrodes. Domain patterns revealed by etching and visualized by optical microscopy.

The wall's coalescence scenario at $\mathbf{Z^+}$ surface is drastically different due to very slow screening between the electrodes. Just before coalescence the narrow residual domain starts to "tear" in dashes and dots (Fig. 7b).

4. *IN SITU* OBSERVATION OF DOMAIN KINETICS

4.1. Instantaneous domain patterns in lithium niobate

The direct observation of the domain kinetics during switching has been used for detail studying of the domain structure evolution in LN (Fig. 8). We have obtained the hexagon domain shape. One can see the pronounce irregularities in wall propagation and its interaction with individual arisen domains. Moreover the preferential orientation of the walls is brightly demonstrated from the beginning to the end of switching.

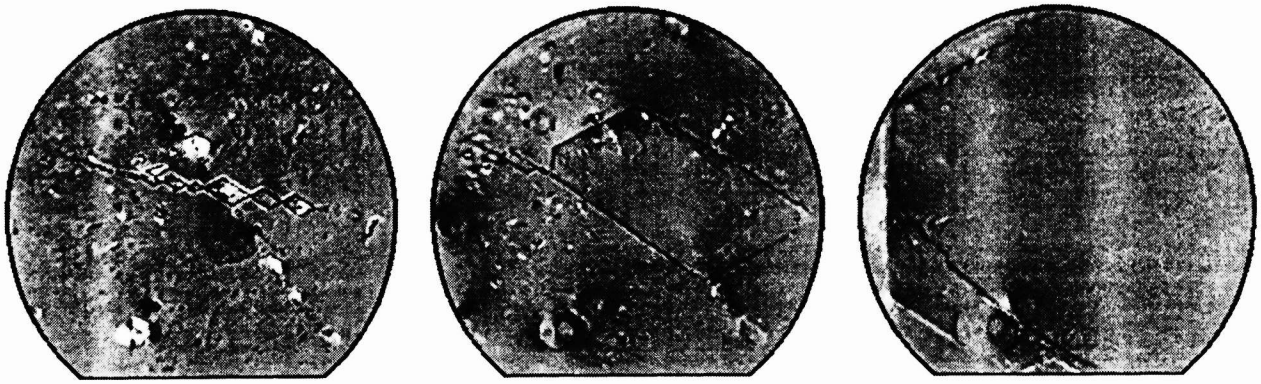

(a) (b) (c)

Fig. 8 Evolution of domain structure during repoling in uniform external field in LN. Diameter of poling area 1 mm, E = 15.3 kV/mm.

The typical evolution of the domain structure in LN is the nucleation along the edges of electrodes and propagation of the formed domain walls to the center of the switching area. Another scenario was obtained in the samples with surface defects. In the case shown at Figure 8 we choose the special crystal area with small scratch in the center. Such artificial nucleation sites leads to start of switching in the center and domain growth to the boundaries of the switched area. The domain shape is far from the regular hexagons but all domain walls are oriented along **Y** directions. Any local deviation from the allowed crystallographic orientations rapidly disappears. The domain growth is usually connected with the propagation of microscale domain steps along the wall.

In situ domain observation opens the possibility to measure directly the average sideways wall motion velocity and its field dependence (Fig. 9). It was shown that experimental data measured in wide velocity range could be fitted by conventional field dependence

$$V(E) = V_\infty \exp[E_{ac}/(E - E_{th})]. \qquad (3)$$

The threshold field $\mathbf{E_{th}}$ averaged over sample area for poling is 17.8 kV/mm and for repoling - 14.0 kV/mm.

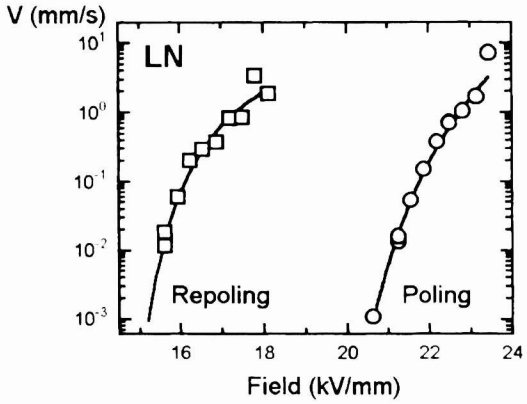

Fig. 9 Field dependence of the average velocity of the domain wall motion in LN. Experimental points are fitted by Equation (3).

4.2. Instantaneous domain patterns in lithium tantalate

The main features of the domain evolution in LT are similar to that in LN. But the nucleation along the edges of electrodes in LT is negligible and the density of arising domains is about 1000 mm^{-2} (Fig. 10a). In this case the shape of growing domains is more irregular due to permanent merging of the moving walls with individual domains. The clear tendency to reconstruct the regular shape of domains after merging is also obtained. The significant difference in domain evolution scenarios between LT and LN is connected with coexistence of "fast-growing" and "slow-growing" domains in LT (Fig. 10). The small slow-growing domains appear at the very beginning of the switching process (Fig. 10a) and then enlarge extremely slow. The fast-growing domains are formed as a result of merging of the closest neighbor small domains (Fig. 10b). Sideways wall motion of fast-growing domain represents the sequence of step generation acts through wall merging with slow-growing domains (Fig. 10b,c). The arisen steps propagate rapidly along the wall.

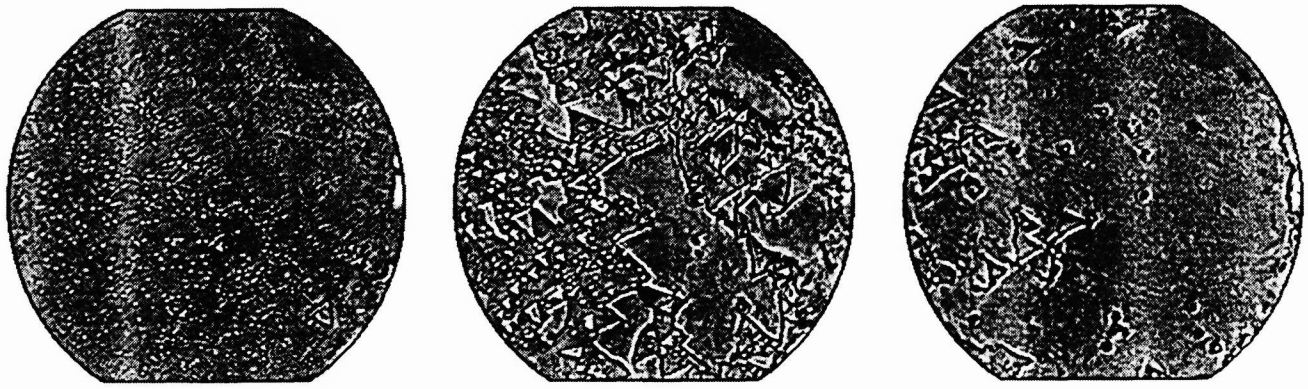

(a) (b) (c)

Fig. 10 Evolution of domain structure during poling in uniform external field in LT. Diameter of poling area 1 mm, E = 19.2 kV/mm.

5. FREQUENCY MULTIPLICATION OF PERIODICAL DOMAIN PATTERNS

We have studied in details the special process of domain evolution during backswitching, which leads to spatial frequency multiplication of domain pattern as compare with the electrode one. The mechanism of frequency multiplication is based on the nucleation along the electrode edges during backswitching (Fig. 11a), while the role of the wall motion in this case is negligible.

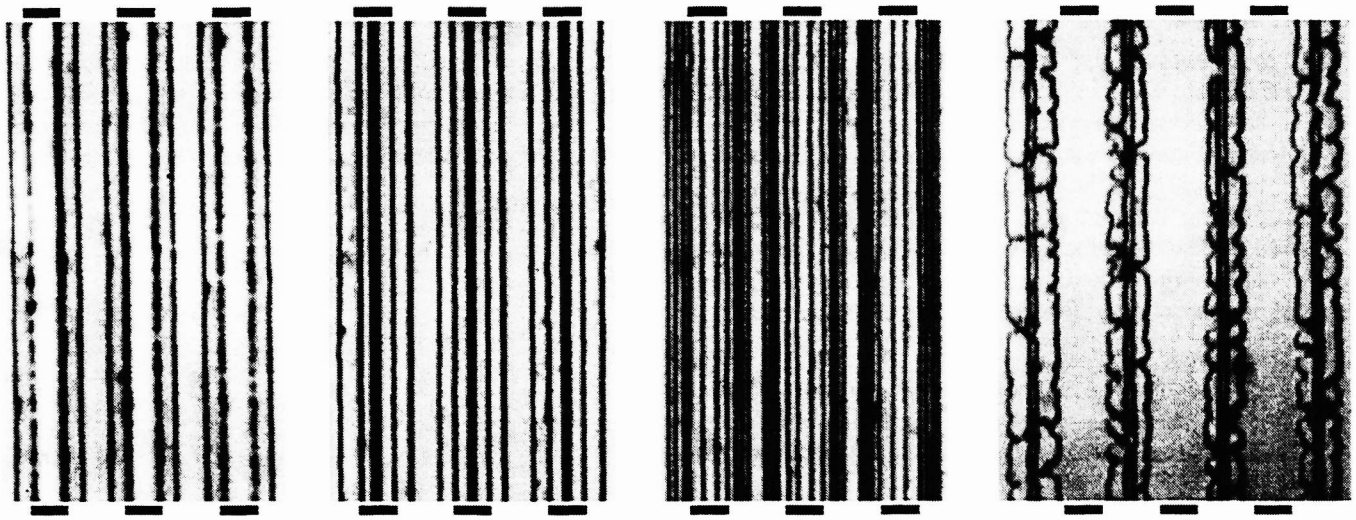

(a) (b) (c) (d)

Fig. 11 Stages of domain evolution during domain frequency multiplication process in LN. Z^+ view. Domain patterns revealed by etching and visualized by optical microscope.

For "frequency tripling" (Fig. 11) the subsequent growth and merging of nucleated domains lead to formation of a couple of strictly oriented sub-micron-width domain stripes under each electrode (Fig. 12, 13a). The width of the stripes increases during backswitching and can be controlled by duration of backswitching stage. The typical depth of the backswitched domain stripes is about 20 - 50 μm (Fig. 13b). It is clear that this structure can be produced only using wide enough electrodes.

For narrow electrodes and long enough backswitching time these stripes merge and only the "frequency doubling" can be obtained (Fig. 13c). The depth of backswitched domain stripes for doubling is typically about 50 - 100 μm (Fig. 13d). The final stage of backswitching presents the merging of wide backswitched domains with residual ones (Fig. 11d). Finally it leads to formation of single domain state, just as before switching.

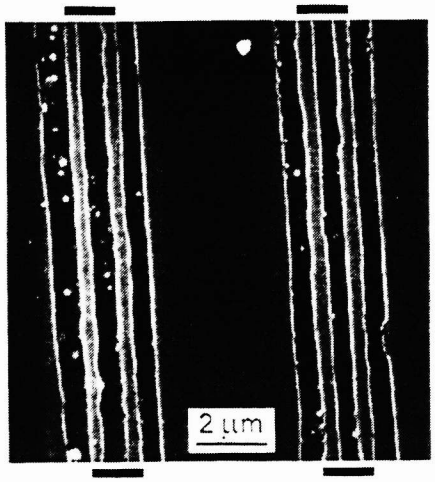

Fig. 12 SEM image of domain "frequency tripling" in LN. Z^+ view.

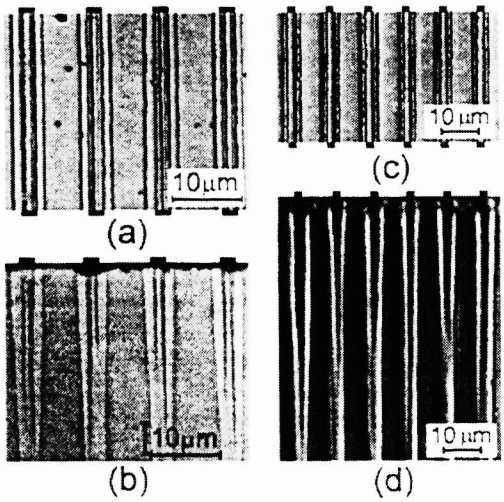

Fig. 13 Domain frequency multiplication in LN. "Frequency tripling": (a) - Z^+ view and (b) - **Y** view. "Frequency doubling": (c) - Z^+ view and (d) - **Y** view. Patterns revealed by etching and visualized by optical microscope.

6. NANODOMAIN ENGINEERING IN LITHIUM NIOBATE

We discovered that the evolution of domains during backswitching in LN is a highly organized process.[11] This spontaneous decay of laminar domain structure proceeds through arising and growth of oriented nanoscale domain arrays contrary to expected trivial backward motion of the existing domain walls accompanied by random nucleation of new domains. Domain evolution during backswitching strongly depends on the value of domain wall shift out of electroded area during "high field" stage. Moreover such parameters of voltage waveform as duration of "high field" stage Δt_{sp} and the value of the jump from "high" to "low" field (field-diminishing amplitude) ΔE allow to control the backswitching kinetics. Three main scenarios of highly organized domain evolution can be revealed (Fig. 14-16).

6.1. Formation of periodic strip nanodomain structures

In the samples with large period of electrode structure (more than 7 μm) for long switching pulse $\Delta t_{sp} \sim 15$ ms the wall shift out of electroded area exceeds 3 μm. In this case for high field-diminishing amplitude $\Delta E \sim 20$ kV/mm the backswitching leads to the formation of the periodic strip domains oriented along the electrodes (Fig. 14). Formation of this structure starts with arising of a couple of 1D-nanodomain arrays strictly under the electrode edges (Fig. 14a). Image processing demonstrates the strong correlation of spatial distribution of arisen nanodomains (average distance between neighbors is about 200 nm). These arrays turn into a pair of strip domains through growth and merge of nanodomains (Fig. 14b). After their complete merging a new couple of 1D-nanodomain arrays appears in nonelectroded area parallel to the first one at the distance about 1 μm (Fig. 14c). On this way it is possible to observe

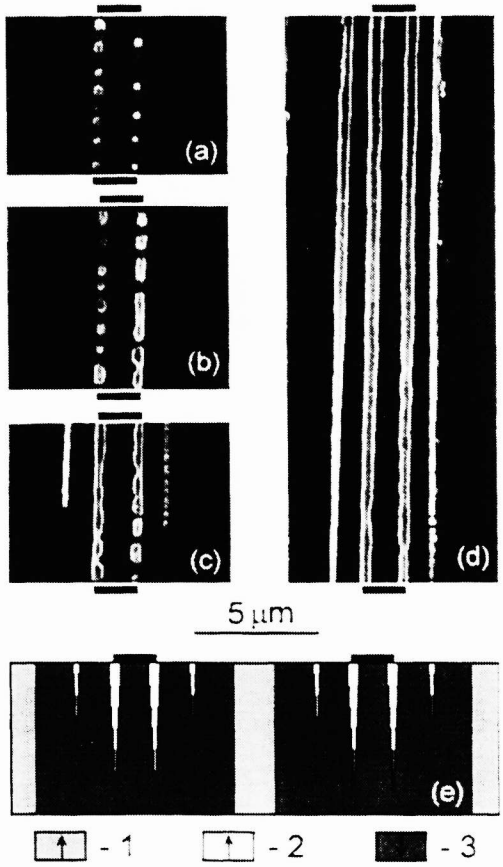

Fig. 14 (a-d) SEM images demonstrating the formation of periodic strip backswitched domains along electrode edges. Top view. (e) Cross-section of domain pattern corresponding to stage (d) (schematical illustration). 1 - non-switched domains, 2 - backswitched domains, 3 - switched domains.

the "frequency pentaplication" effect (Fig. 14c). The distance between secondary and initial stripes is about the thickness of the artificial insulating layer. Therefore we can change the period of the structure by controlled variation of the thickness of insulating layer.

6.2. Formation of the quasi-periodical structure of oriented nanodomain arrays

Spontaneously arisen domain structure for short electrode periods (less than 4 μm) is drastically different. Domain patterns visualized by SEM and SFM demonstrate the highly organized quasi-periodical structure of domain arrays (Fig. 15, 16). Each array is always oriented along determined crystallographic direction. Two variants of array orientation have been obtained under different switching conditions.

For short switching pulse duration Δt_{sp} ~ 5 ms and the low field-diminishing amplitude ΔE ~ 2 kV/mm the domain arrays are oriented strictly in one of three **Y** directions (Fig. 15) at 60 degrees to the electrode edges. Each quasi-regular array is comprised of the nanoscale domains with diameters 30-100 nm and average linear density exceeding $10^4 mm^{-1}$. In contrast to large electrode periods the nucleation along the electrode edges has been never observed.

For long switching pulse duration Δt_{sp} ~ 5 ms and the high field-diminishing amplitude (ΔE > 10 kV/mm) the domain arrays are oriented strictly in one of six **X** directions (Fig. 16). The individual nanoscale domains are triangular shaped and their sizes are about 30-100 nm. In addition the nucleation along the electrode edges and consequent formation of strip domains are observed.

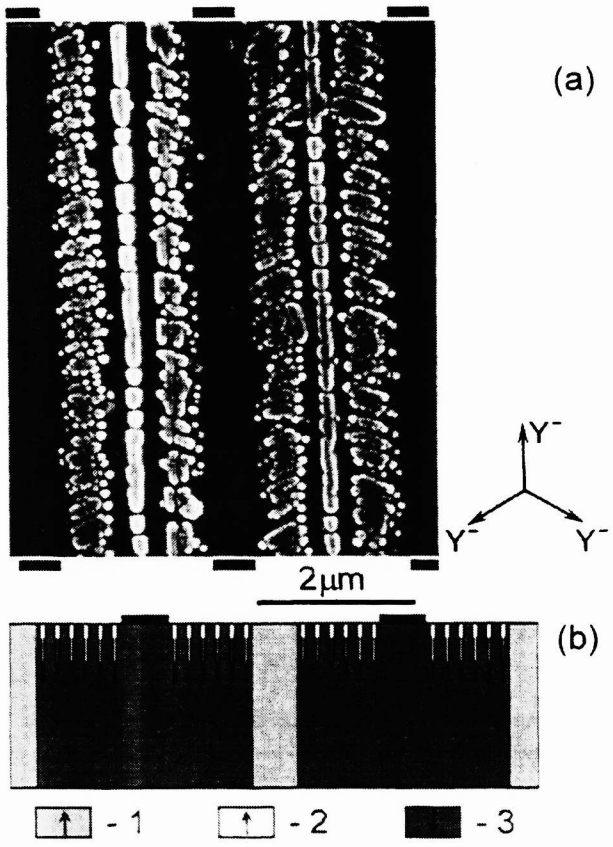

Fig. 15 (a) SEM image of nanodomain arrays oriented along **Y**⁻ directions at 60 degrees to the electrode edges. **Z**⁺ view. Black rectangles show the positions of the electrodes. Domain patterns revealed by etching. (b) The pattern cross-section (schematical illustration). 1 - non-switched domains, 2 - backswitched domains, 3 - switched domains.

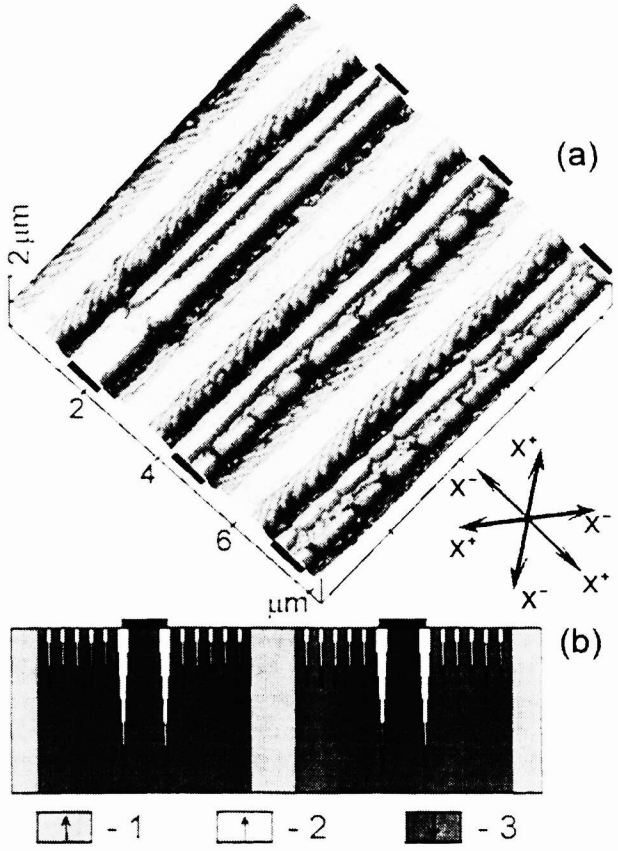

Fig. 16 (a) SFM image of nanodomain arrays oriented along **X** directions at 30 and 90 degrees to the electrode edges. **Z**⁺ view. Black rectangles show the positions of the electrodes. Domain patterns revealed by etching. (b) The pattern cross-section (schematical illustration). 1 - non-switched domains, 2 - backswitched domains, 3 - switched domains.

6.3. Physical basis of nanodomain engineering

All observed results can be explained under the preposition that the switching process in the given place is driven by the polar component of the local electric field $\mathbf{E}_z$. The value of local field $\mathbf{E}_z$ depends on the instantaneous domain pattern and screening degree. $\mathbf{E}_z$ is defined by the sum of polar components of external field $\mathbf{E}_{ex}$, depolarization field $\mathbf{E}_{dep}$ and various screening fields $\mathbf{E}_{scri}$

$$E_z(r,t) = E_{ex}(r) - E_{dep}(r,t) - \Sigma E_{scri}(r,t) \quad (4)$$

In the case of strip electrodes $\mathbf{E}_{ex}$ is essentially inhomogeneous with strong increase in the surface layer along the electrode edges due to the fringe effect. The depolarization field $\mathbf{E}_{dep}$ is produced by bound charges and always hampers the domain growth. It tends to reconstruct the initial domain pattern when the $\mathbf{E}_{ex}$ is switched off. It is clear that for multi-domain state $\mathbf{E}_{dep}$ is essentially inhomogeneous. Both fields are compensated by screening processes.

Just after switching the current in the external circuit mainly screens the arising $\mathbf{E}_{dep}$ (external screening). The degree of fast screening and therefore the value of residual depolarization field depend on the ratio between thickness of sample and dielectric layer (Fig. 17a)[12]

$$E_{rdep} = L/d\ Ps/\varepsilon\varepsilon_o. \quad (5)$$

In used experimental geometry (Fig. 17a) the thickness of dielectric layer is spatially nonuniform. Under the electrodes the thickness is determined by the sub-micron intrinsic layer (dead layer) $\mathbf{L}_{in}$ and out of electrodes by deposited 0.5 μm-thick isolating layer $\mathbf{L}_{is}$.

The bulk screening processes compensate the residual part of the local field $\mathbf{E}_{zr}$

$$E_{zr}(r,t) = E_{ex}(r) - (E_{dep}(r,t) - E_{screx}(r,t)) \quad (6)$$

In wide switched domain (Fig. 17b) the $\mathbf{E}_{zr}$ under the electrodes is much less than out of electroded area since $\mathbf{L}_{in} << \mathbf{L}_{is}$.

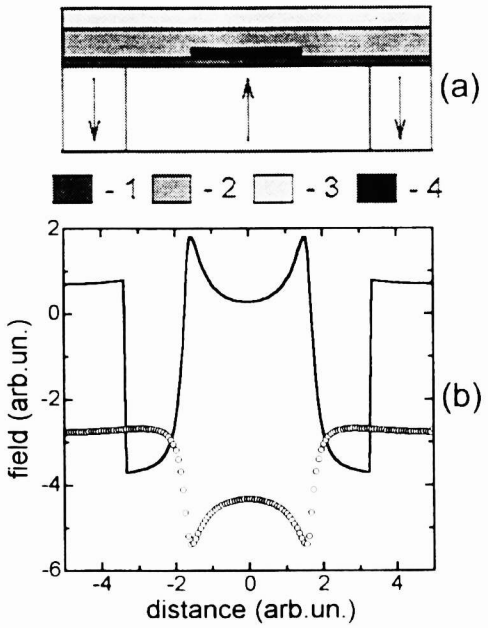

Fig. 17 (a) Surface region of the substrate with strip electrode: 1 - dielectric gap, 2 - insulating layer, 3 - liquid electrolyte, 4 - metal electrode. (b) Calculation of the spatial distribution of backswitching field near $\mathbf{Z}^+$ surface: in two limiting cases (solid line - low ΔE and short switching pulse Δt_{sp}, points - high ΔE and long Δt_{sp}).

The bulk screening process is slower and determined by redistribution of bulk charges, reorientation of the defect dipoles and injection from electrodes through the insulating layer during switching.[10,12] As a result the field spatial distribution after removing of external field depends on the duration of switching pulse and field decreasing amplitude (Fig. 1b).

6.4. Correlated nucleation under the electrode edges

In order to explain why the nucleation starts under the electrode edges we calculate the spatial distribution of field polar component of $\mathbf{E}_Z$ in sample with periodical electrodes (Fig. 18). As it was anticipating this distribution demonstrates sharp singularities under the edges of finite electrodes. It must be pointed out that spatially nonuniform $\mathbf{E}_Z(x,y)$ exists only in the vicinity of the surface and its amplitude rapidly decreases with the depth (Fig. 18). Practically uniform field is obtained at the depth about the electrode period. Such estimations clarify the cause of observed spatially nonuniform nucleation in thin surface layer and show that subsequent growth of domains in the bulk goes on in uniform electric field.

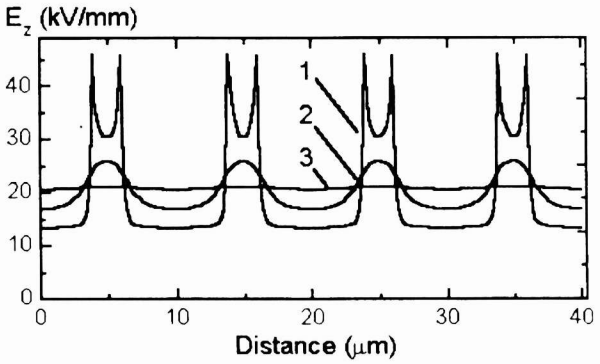

Fig. 18 Calculated spatial distribution of field polar component $\mathbf{E}_Z$ near $\mathbf{Z}^+$ surface in sample with periodical electrodes.

6.5. Mechanism of correlated nucleation

It is obvious that understanding of correlated nucleation mechanisms needs the knowledge of spatial distribution of the local field polar component. We suppose that the peculiarities of external screening play a principal role in this effect. In order to verify this hypothesis the spatial distribution of local field produced by individual strip nonthrough domain located at the surface was calculated for the infinite plate completely covered by uniform electrodes (Fig. 19). The maximums of residual depolarization field E_{dr} are observed at the distance of about thickness of dielectric gap L from domain wall (Fig. 19, 20a).

It was found from this calculation that local field maximums exist only near the surface just under the dielectric gap and disappear at the depth of the order of L (Fig. 20a,b). The value of maximum decreases proportionally to the reciprocal value of the depth (Fig. 20b) and the distance from the domain wall to field maximum linearly increases with depth (Fig. 20c). These results allow to explain the effect of correlated nucleation. It is clear that the position of the nucleation site must correspond to the field maximum because the local field near the surface determines the nucleation probability. Many evidences of correlated nucleation were observed in LN during switching in uniform field. One of the common manifestations of this effect is the arising of the nuclei at short distance from the plane domain wall. It was shown also that the correlated nucleation plays important role during backswitching.

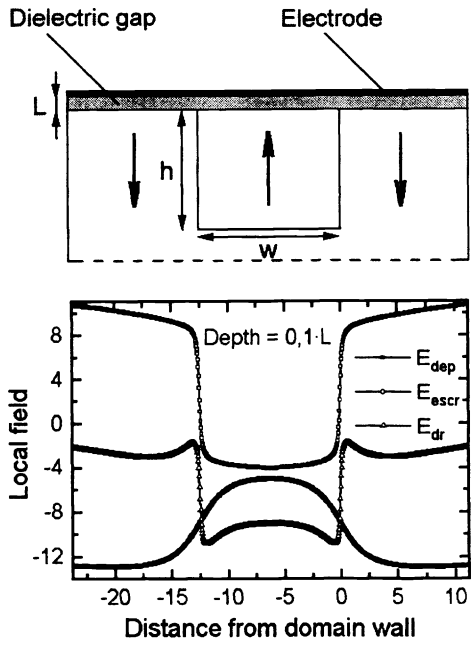

Fig. 19 Scheme of the surface layers and the spatial distribution of depolarization and screening fields caused by strip domain. Distance from the domain wall and depth from the dielectric gap are given in units of dielectric gap thickness L. Domain sizes h = w =12.5·L.

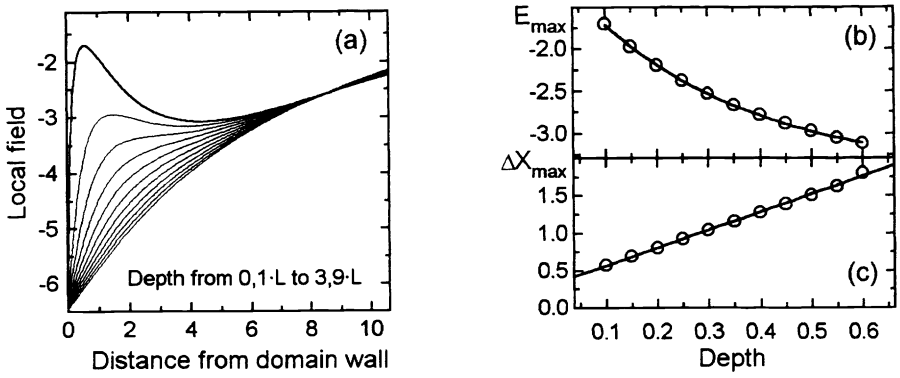

Fig. 20 (a) Change of spatial distribution of the local field produced by strip domain for different depth from the dielectric gap. (b) Dependence on the depth of local field maximum and (c) the distance from the position of local field maximum to the wall.

7. APPLICATION OF THE BACKSWITCHED POLING FOR 2.6 μm PATTERNING

We have applied the backswitching method for 2.6-μm periodical poling of the LN 0.5-mm-thick substrates. It is seen that the domain patterns on Z^- are practically ideal (Fig. 21). Such domain structure was prepared in fragments of 3-inch-diameter substrate. It must be pointed out that to our knowledge all to date attempts to produce the periodic domain structures with such period in 0.5-mm-thick LN by conventional poling method have not met with success.

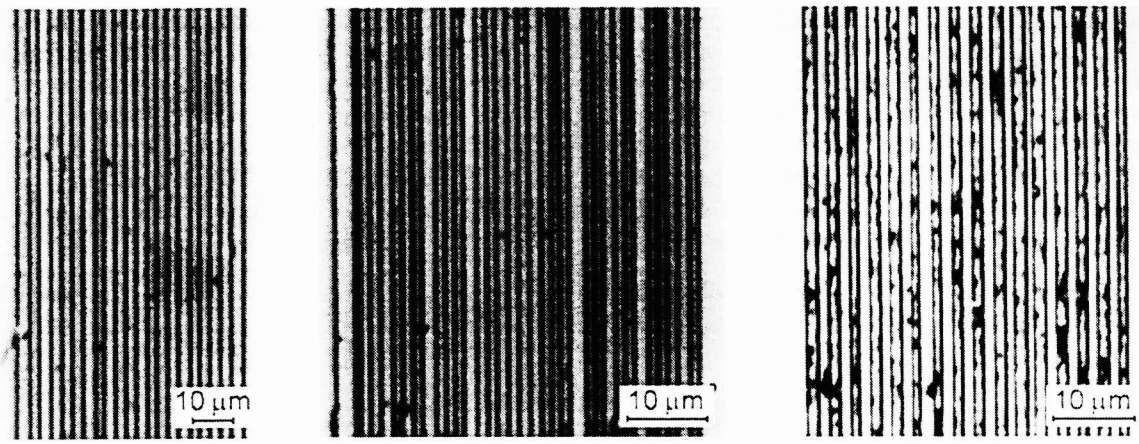

Fig. 21 Domain patterns in LN for 2.6 μm period for Z^- view revealed by etching were visualized by optical microscopy.

7.1. Quasi-phasematched generation in backswitched-poled lithium niobate

The continuous-wave single-pass second harmonic generation in 4-μm-period 0.5-mm-thick backswitched-poled LN was obtained.[5,7,13] Using this material, 50-mm-length devices where characterized for continuous wave (CW) single-pass second harmonic generation of blue light.[14] Using the CW Ti:sapphire pump laser near confocally focused to a 44 μm waist radius in the center of the sample, 6.1%/W efficient first-order generation of 61 mW at λ = 460 nm was achieved, indicating an effective nonlinearity $d_{eff} \approx$ 9pm/V, approximately one half of the nominal value. The obtained nearly ideal tuning curve for 460 nm second harmonic generation phase matching versus temperature, indicating that the sample phase matches nominally over the full 50 mm length.[14]

Moreover laser-diode-pumped second harmonic generation was performed with an antireflection-coated InGaAs single-stripe diode master oscillator (SDL prototype) in a Littman external-cavity configuration.[15] The oscillator was single frequency and tunable from 874 to 936 nm, with maximum output of 20 mW at 930 nm. The pump power after the amplifier and two pairs of optical isolators was more than 2 W. With 1.5 W of laser-diode power, 60 mW of second harmonic generation at 465 nm was produced, given a normalized conversion efficiency of 2.8%/W. An improved efficiency of 3.4%/W was obtained by expansion and spatial filtering of the diode beam before it was focused into the periodically poled LN.[15]

7.2. 2.6 μm patterning in lithium tantalate

We have applied the optimized method for 2.6-μm periodical poling of the LT 0.3-mm-thick substrates. It is seen that the domain patterns on Z^+ are practically ideal (Fig. 22). Such domain structure was prepared in fragments of 2-inch-diameter substrate. The detail optical testing of the obtained domain structures will be done later.

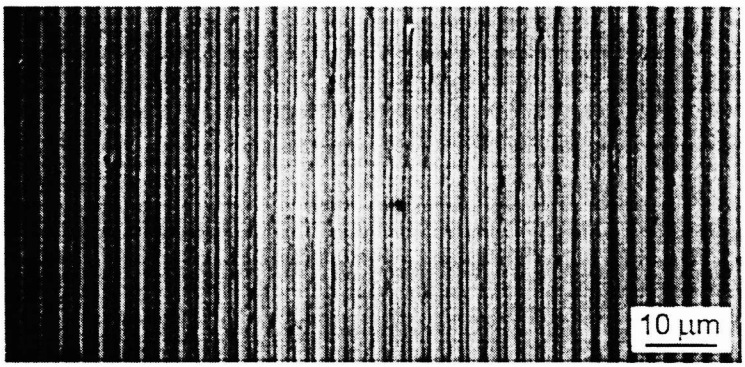

Fig. 22 Domain patterns in LT for 2.6-μm-period for Z^+ view revealed by etching and visualized by optical microscopy.

The new important information about the domain kinetics in congruent and stoichiometric LN and LT during backswitched poling was obtained as a result of aforementioned investigations. The real-time observation of the domain kinetics during poling in both crystals is a new powerful instrument for optimization of the poling technique. The modified poling process allowed to produce for the first time the bulk domain patterns with 2.6-μm-period in 0.5-mm-thick LN and 0.3-mm-thick LT substrates. It was shown that backswitched poling enables higher fidelity and shorter period domain patterning. The proposed technology based on the controlled backswitching process demonstrates the new possibilities in the domain engineering. The first achievements in domain frequency multiplication and nanodomain engineering show the way to overcome the micron-period barrier in domain patterning.

The future progress in periodical patterning requires the development of such activity for patterning of thicker substrates of stoichiometric and doped LN and LT produced by different techniques.

ACKNOWLEDGMENTS

The research was made possible in part by Program "Basic Research in Russian Universities" (Grant No.5563), by Grant No.97-0-7.1-236 of the Ministry of Common and Professional Education of the Russian Federation, by Grant No.98-02-17562 of the Russian Foundation of Basic Research, by the EOARD, Air Force Office of Scientific Research, AFRL, under Contract No.F61775-99-WE037 and by TRW Foundation, CNOM, and AVLIS Program - Lawrence Livermore National Laboratory, and by General Motors Fellowship supporting the work of GDM.

REFERENCES

1. R.L. Byer, "Quasi-phasematched nonlinear interactions and devices ", *J. of Nonlinear Optical Physics & Materials* **6**, pp. 549-592, 1997.
2. M. Yamada, N. Nada, M. Saitoh, and K. Watanabe, "First-order quasi-phase matched $LiNbO_3$ waveguide periodically poled by applying an external field for efficient blue second-harmonic generation", *Appl.Phys.Lett.* **62**, pp. 435-436, 1993.
3. L.E. Myers, R.C. Eckardt, M.M. Fejer, R.L. Byer, and W.R. Bosenberg, "Multigrating quasi-phase-matched optical parametric oscillator in periodically poled $LiNbO_3$", *Optic Lett.* **21**, pp. 591-593, 1996.
4. G.D. Miller, R.G. Batchko, M.M. Fejer, and R.L. Byer, "Visible quasi-phasematched harmonic generation by electric-field-poled lithium niobate", *SPIE Proc. on Solid State Lasers and Non-linear Crystals* **2700**, pp. 34-45, 1996.
5. V.Ya. Shur, R.G. Batchko, E.L. Rumyantsev, G.D. Miller, M.M. Fejer, and R.L. Byer, "Domain engineering: periodic domain patterning in lithium niobate", *Proc. 11th ISAF*, (Piscataway, NJ: IEEE, 1999), pp. 399-406.
6. V. Shur, E. Rumyantsev, R. Batchko, G. Miller, M. Fejer, and R. Byer, "Physical basis of the domain engineering in the bulk ferroelectrics", *Ferroelectrics* **221**, pp. 157-167, 1999.
7. R.G. Batchko, V.Ya. Shur, M.M. Fejer, and R.L. Byer, "Backswitch poling in lithium niobate for high-fidelity domain patterning and efficient blue light generation", *Appl.Phys.Lett.* **75**, pp. 1673-1675, 1999.
8. V.Ya. Shur, E.L. Rumyantsev, R.G. Batchko, G.D. Miller, M.M. Fejer, and R.L. Byer, "Domain kinetics during periodic domain patterning in lithium niobate, *Phys. Solid State* **41**, pp. 1681-1687, 1999.
9. V.Ya. Shur, A.L. Gruverman, V.V. Letuchev, E.L. Rumyantsev, and A.L. Subbotin, "Domain structure of lead germanate", *Ferroelectrics* **98**, pp. 29-49, 1989.
10. V.Ya. Shur, in *Ferroelectric Thin Films: Synthesis and Basic Properties*, ch. 6, Gordon&Breach, New York, 1996.
11. V.Ya. Shur, E.L. Rumyantsev, E.V. Nikolaeva, E.I. Shishkin, D.V. Fursov, R.G. Batchko, L.A. Eyres, M.M. Fejer, and R.L. Byer, "Nanoscale backswitched domain patterning in lithium niobate", *Appl.Phys.Lett.* **76**, pp. 143-145, 2000.
12. V.M. Fridkin, *Ferroelectrics Semiconductors*, ch. 3, Consultants Bureau, New York and London, 1980.
13. R.G. Batchko, G.D. Miller, V.Ya. Shur, E.L. Rumyantsev, M.M. Fejer, and R.L. Byer, "Domain patterning in lithium niobate using spontaneous backswitching", *SPIE Proc. on Laser Material Crystal Growth and Nonlinear Materials and Devices* **3610**, pp. 36-43, 1999.
14. R.G. Batchko, M.M. Fejer, R.L. Byer, V.Ya. Shur, and L. Erman, "Backswitch poling of 0.5-mm-thick lithium niobate for 6.4%/W-efficient cw second harmonic generation of 460 nm light", *OSA Trends in Optics and Photonics Series* **26**, Advanced Solid-State Lasers, M.M. Fejer, H. Injeyan and U. Keller (eds.), pp. 707-708, 1999.
15. R.G. Batchko, M.M. Fejer, R.L. Byer, D. Woll, R. Wallenstein, V.Ya. Shur, and L. Erman, "Continuous-wave quasi-phase-matched generation of 60 mW at 465 nm by single-pass frequency doubling of a laser diode in backswitch-poled lithium niobate", *Opt.Lett.* **24**, pp. 1293-1295, 1999.